Received: 19 March 2018 | Revised: 3 June 2018 | Accepted: 8 June 2018
DOI: 10.1002/ardp.201800083

FULL PAPER

DPhG ARCH PHARM
Archiv der Pharmazie

Identification of pyrazolopyridine derivatives as novel spleen tyrosine kinase inhibitors

Yahui Huang | Yu Li | Guoqiang Dong | Wannian Zhang | Na Liu | Chunquan Sheng

School of Pharmacy, Second Military Medical University, Shanghai, People's Republic of China

Correspondence
Prof. Chunquan Sheng and Na Liu, School of Pharmacy, Second Military Medical University, 325 Guohe Road, Shanghai 200433, People's Republic of China.
Email: shengcq@smmu.edu.cn (C.S.), liuna66@aliyun.com (N.L.)

Funding information
The National Key R&D Program of China, Grant number: 2017YFA0506000; National Basic Research Program of China, Grant number: 2014CB541800

Abstract

Inhibition of spleen tyrosine kinase (Syk) is a promising strategy for the treatment of various allergic and autoimmune disorders such as asthma, rheumatoid arthritis, and allergic rhinitis. Previously, a Syk inhibitor with novel indazole scaffold was discovered by structure-based virtual screening. Herein, the structure–activity relationship of the indazole Syk inhibitors was investigated. Several new inhibitors demonstrated potent activity against Syk. In particular, compound **18c** showed good Syk inhibitory activity (IC_{50} = 1.2 μM), representing a good lead compound for further optimization.

KEYWORDS
pyrazolopyridines inhibitors, spleen tyrosine kinase, structure–activity relationship, structure-based drug design

1 | INTRODUCTION

Inflammation is generally the body's first immune response to irritation and infection, which can be classified into acute inflammation and chronic inflammation. The latter is the result of many autoimmune and inflammatory diseases (e.g., rheumatoid arthritis, RA), which is the consequence of imbalance between the innate and the adaptive immune system. Although non-steroidal anti-inflammatory drugs (NSAIDs) and disease-modifying antirheumatic drugs (DMARDs) are widely used in the treatment of pain and inflammation, long-time use usually results in adverse side effects.[1,2] Therefore there is an urgent need for novel therapeutics with better pharmacological features. Recently, progress in the signal path of autoimmune and allergic diseases has identified several new targets,[3] and spleen tyrosine kinase (Syk) is one of them with promising therapeutic value.

Syk, a member of the non-receptor protein tyrosine kinase family, is mainly expressed in hematopoietic cells, including B cells, mast cells, macrophages, and neutrophils.[4] Syk plays a key role in coupling activated immunoreceptor to downstream events which orchestrates various cellular responses (e.g., proliferation, differentiation, cell adhesion, cytokine production, mast cell degranulation). Thus, targeting Syk is a promising strategy for the treatment of inflammatory and autoimmune disorders.[5] To date, a number of Syk inhibitors were developed for treating various diseases ranging from arthritis to leukemia. Fostamatinib (**2**, Figure 1) is a prodrug of R406 (**1**) and has demonstrated efficacy in several animal models including RA,[6] nephrotoxic nephritis,[7] asthma,[8] systemic lupus erythramatosis (SLE),[9] autoimmune diabetes,[10] and autoimmune hemolytic anemia (AHA).[11] However, compound **2** failed in phase 3 clinical trials because of severe side effects,[12,13] which putatively attributed to the poor kinase selectivity of its parent compound **1**.[14] A more selective inhibitor **3** (Figure 1) is currently in phase 2 clinical trials, but safety data have not yet been reported. Previously, we identified compound **4** as a novel Syk inhibitor through structure-based virtual screening.[15] However, its Syk inhibitory activity remains to be further improved and its structure–activity relationship (SAR) is still unknown. Therefore, a series of novel indazole Syk inhibitors were rationally designed, synthesized, and assayed.

Yahui Huang and Yu Li contributed equally to this work.

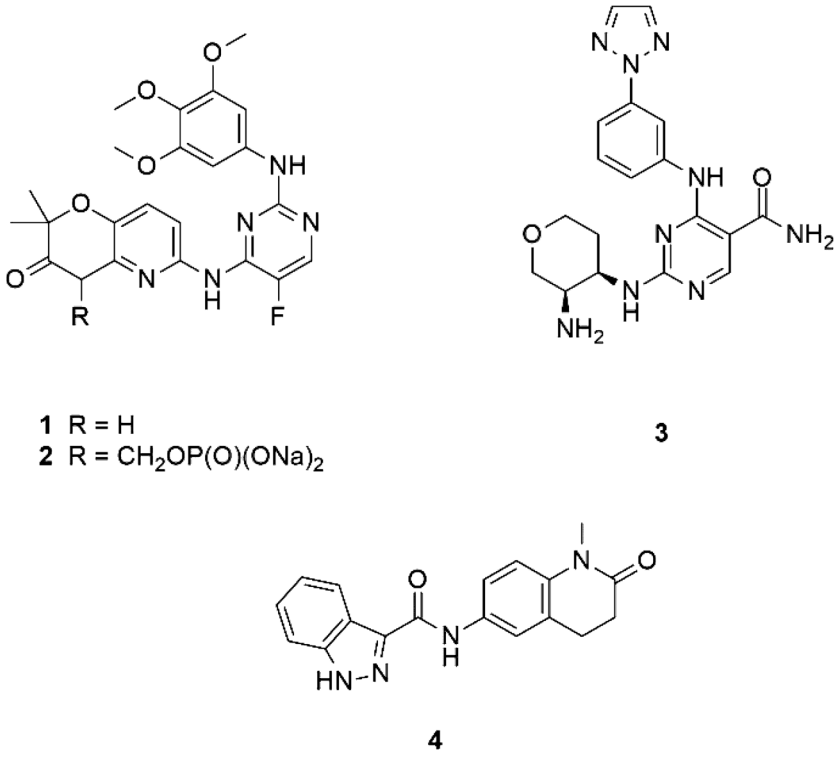

FIGURE 1 Chemical structures of the Syk inhibitors

2 | RESULTS AND DISCUSSION

2.1 | Design rationale

As shown in Figure 2, the superposition of binding conformation of compounds **1** and **4** was performed to guide structural modification of compound **4**. On the basis of the binding mode, a series of pyrazolopyridine inhibitors were rationally designed (Figure 3). First, aromatic groups were introduced on the indazole scaffold to form additional hydrophobic interactions with Syk. Second, the replacement of benzene of the indazole by pyridine/pyrazine formed additional hydrogen bond with the Syk hinge region. Third, various amide side chains were designed to adjust the hydrophobic and hydrogen bonding interactions with Syk.

2.2 | Chemical synthesis

The synthetic routes of the target compounds are shown in Schemes 1 and 2. Commercially available compound **5** reacted with hydrazine hydrate under the microwave conditions, affording compound **6** (Scheme 1). Then Suzuki coupling reaction was applied for the synthesis of the key intermediate **8**, which was treated with the substituted carboxylic acids **9** or **10** in the presence of HBTU and Et_3N to give compounds **11a–c** and **12**. Finally, the removal of the Boc protecting group and/or methyl group in the presence of BBr_3 gave target compounds **13a**,**b** and **14a**,**b**. Compounds **18a–e** were synthesized by a similar procedure using compound **15**[16] as the starting material (Scheme 2).

2.3 | Syk inhibitory activity

The Syk inhibitory activities of the target compounds were evaluated using the assay as previously described.[15] As shown in Table 1, various substitutions were introduced on the benzene group including

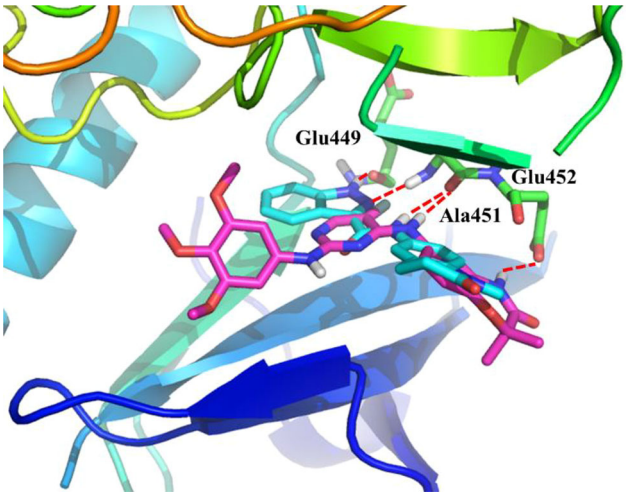

FIGURE 2 Superimposition of the binding conformation of compounds **1** and **4** in the active site of Syk (PDB ID: 3FQS[17]). Compound carbon atoms colored in purple for compound **1** and in cyan for compound **4**. The figure was generated using PyMol (http://www.pymol.org/)

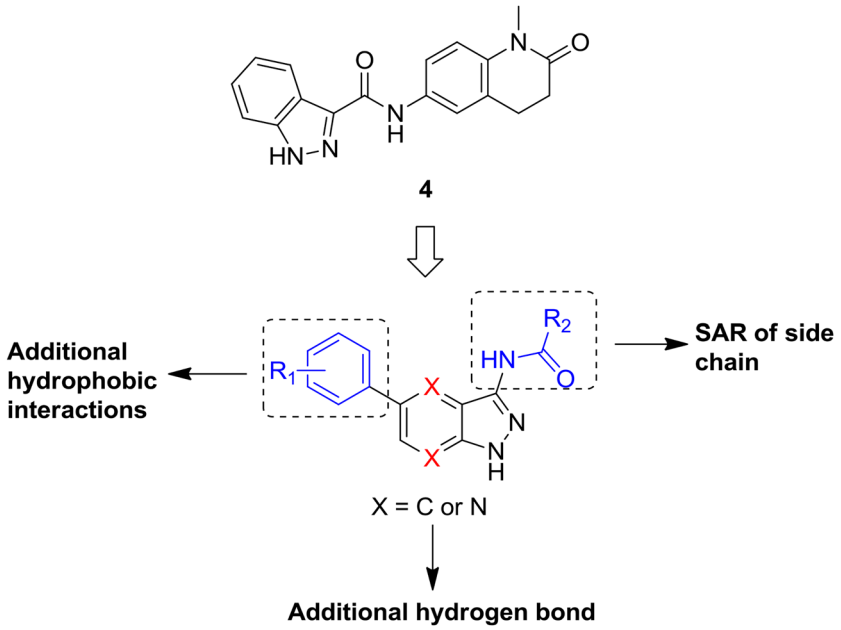

FIGURE 3 Design rationale of the indazole Syk inhibitors

4-fluoro (**11a**), 3-ethyl ester (**11b**, **11c**), 3-amino (**13a**, **13b**) and 3-hydroxyl (**14a**, **14b**) groups with various substituted amides on the indazole scaffold. However, only a few compounds (**11b**, **14a**, and **14b**) showed moderate inhibitory Syk activity at 5 μM.

Owing to the poor activity of the indazole derivatives, the pyrazolopyridine and pyrazolopyrazine derivatives (**18a–e**) were further synthesized and evaluated (Table 2). Interestingly, the pyrazolopyridine analogues (**18a** and **18b**) showed improved activity as compared to the corresponding indazole compounds. Moreover, the introduction of *meta*-benzoic acid (**18c**) led to significant increase of the Syk inhibitory activity (IC_{50} = 1.2 μM), which was more potent compound **4** (IC_{50} = 3.2 μM). Unfortunately, the replacement of pyridine by pyrazine group on the indazole skeleton (**18d** and **18e**) resulted in decreased activity.

2.4 | Molecular docking

Molecular docking studies were performed using GOLD 5.0[18] to investigate the binding mode of compound **18c** with Syk. The crystal structure of Syk in complex with compound **1** was obtained from protein database bank (PDB ID: 3FQS[17]) and prepared for molecular docking analysis in Discovery Studio 3.0. As depicted in Figure 4, the pyrazolopyridine scaffold formed two hydrogen bonds with Ala451 and Glu449 in the Syk hinge region. In contrast, compound **1** only formed a hydrogen bond with Ala451. The 4-fluorophenyl formed hydrophobic and van der Waals interaction with Pro455, which was identified as a reliable residue to achieve high levels of Syk specificity and potency.[19] Moreover, the carboxyl interacted with Asp512 through a hydrogen bond. On the basis of the binding mode and SAR, the three hydrogen bonds were essential for the Syk inhibitory activity.

3 | CONCLUSIONS

In summary, a series of novel indazole, pyrazolopyridine, and pyrazolopyrazine Syk inhibitors were designed and synthesized. Several derivatives exhibited good Syk inhibitory potency. Especially, compound **18c** showed improved inhibitory activity against Syk (IC_{50} = 1.2 μM) compared to the hit compound **4** (IC_{50} = 3.2 μM). Taken together, the present study provides a good starting point for the development of novel Syk inhibitors. Further structural optimization is in process.

4 | EXPERIMENTAL

4.1 | Chemistry

4.1.1 | General procedures

Reagents were purchased from commercial sources and were used without further purification. Oxygen or water sensitive reactions were performed under the nitrogen atmosphere. ^{13}C NMR and ^{1}H NMR spectra were recorded on Bruker AVANCE600, or AVANCE300 spectrometer (Bruker Company, Germany), operating at the indicated frequencies and $CDCl_3$ or DMSO-d_6 as solvents. Chemical shift was expressed in ppm (δ). The mass spectra were recorded on an Esquire 3000 LC-MS mass spectrometer. Flash chromatography was performed on 200–300 mesh silica gel with the indicated solvent systems (Qingdao Haiyang Chemical, China).

The InChI codes of the investigated compounds together with some biological activity data are provided as Supporting Information.

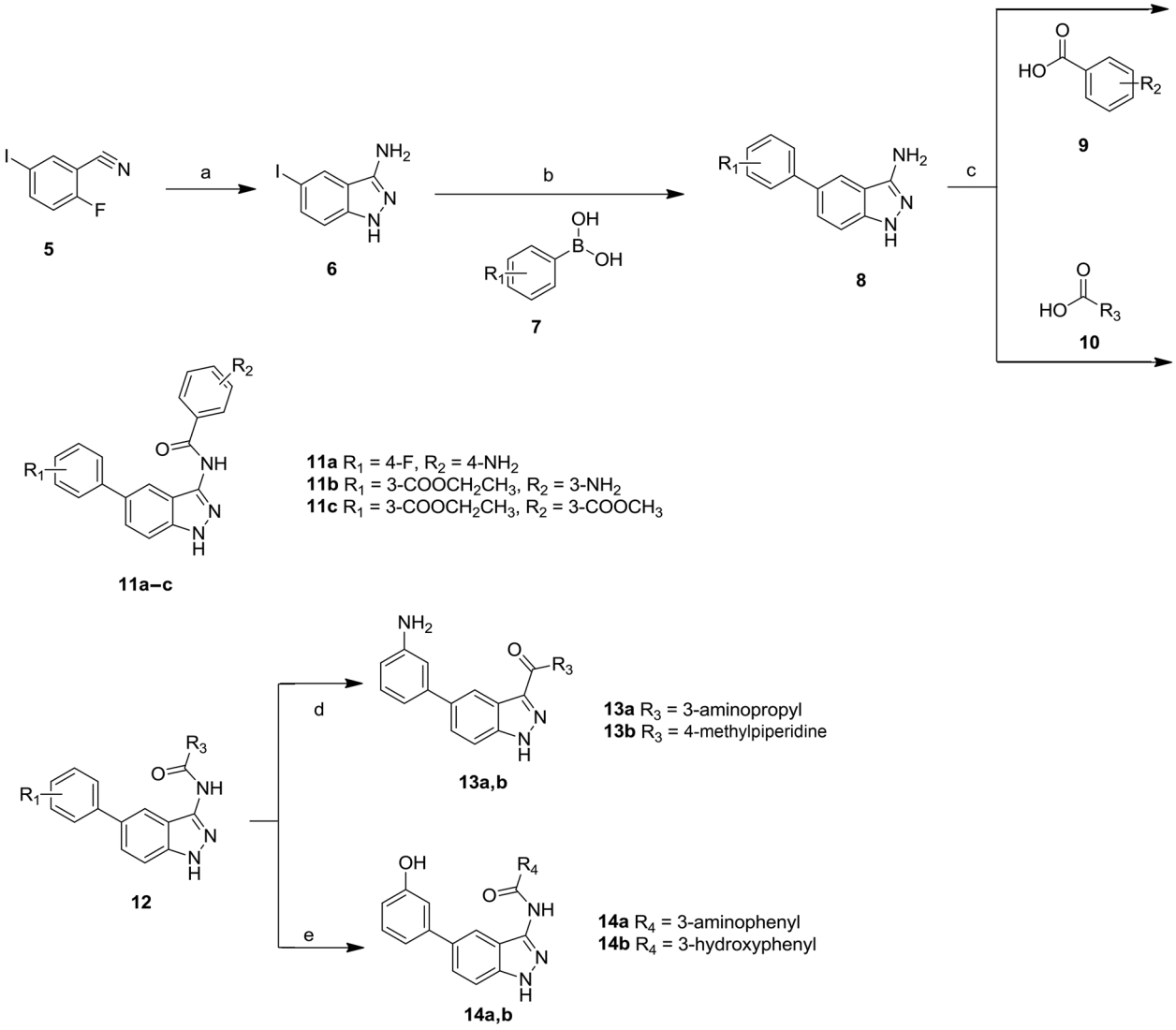

SCHEME 1 Chemical synthesis of compounds **11a–c**, **13a**, **13b**, **14a**, and **14b**. Reagents and conditions: (a) hydrazine hydrate, CH_3CH_2OH, microwave, 150°C, 20 min, 95%; (b) $Pd(PPh_3)_4$, Na_2CO_3, 1,4-dioxane, H_2O, reflux, 12 h, 35%; (c) HBTU, Et_3N, DMF, rt, 2 h, 46–85%; (d) CF_3COOH, CH_2Cl_2, rt, 1 h, 67%; (e) BBr_3, CH_2Cl_2, −78°C, 4 h, 54%

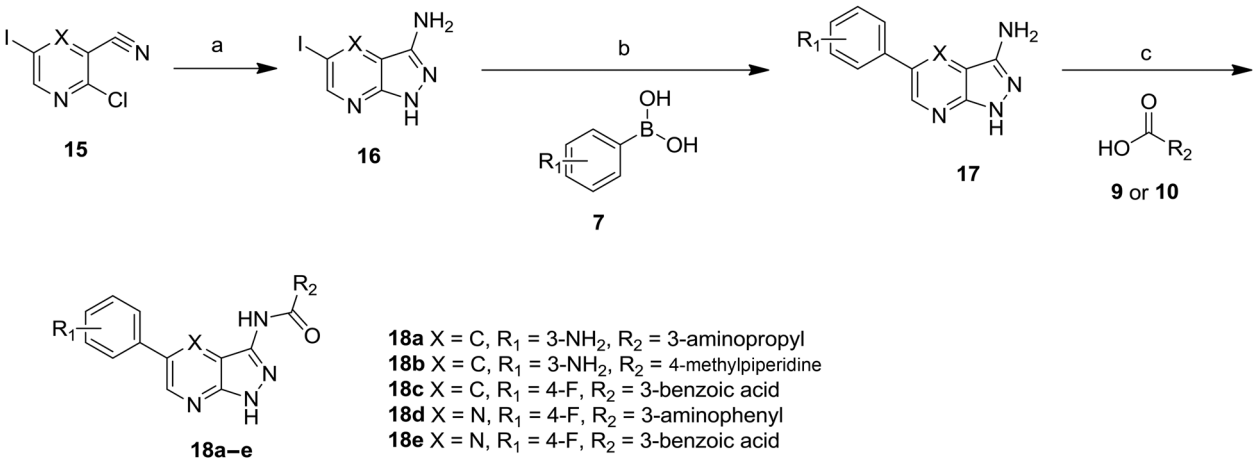

SCHEME 2 Synthesis route for compounds **18a–e**. Reagents and conditions: (a) hydrazine hydrate, CH_3CH_2OH, microwave, 150°C, 20 min, 95%; (b) $Pd(PPh_3)_4$, Na_2CO_3, 1,4-dioxane, H_2O, reflux, 12 h, 35%; (c) HBTU, Et_3N, DMF, rt, 2 h, 46–85%

TABLE 1 Syk inhibition activity of target compounds **11a–c**, **13a**, **13b**, **14a**, and **14b**

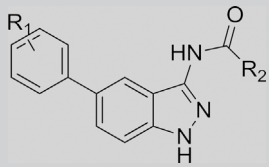

Compound	R_1	R_2	Inhibition rate at 5 μM (%)
11a	4-F	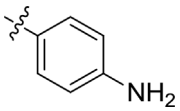	−8.1
11b	3-$COOCH_2CH_3$	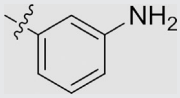	28
11c	3-$COOCH_2CH_3$	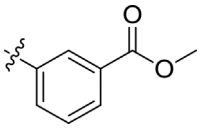	0.2
13a	3-NH_2	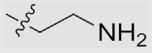	−3.8
13b	3-NH_2	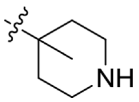	−2.4
14a	3-OH	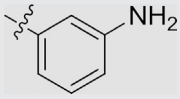	30.0
14b	3-OH	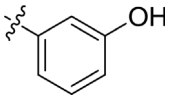	33.7

4.1.2 | Synthetic procedures

4-Amino-*N*-(5-(4-fluorophenyl)-1*H*-indazol-3-yl)benzamide (11a)

A solution of 2-fluoro-5-iodobenzonitrile (**5**, 1.0 g, 4 mmol) and hydrazine hydrate (1 mL) in ethanol (5 mL) was reacted under microwave condition at 150°C for 20 min. The solvent was concentrated *in vacuo*, and the mixture was purified by column chromatography (CH_2Cl_2/CH_3OH = 100:2) to give compound **6** (1.0 g, yield 97%) as off-white solid. A mixture of compound **6** (1.0 g, 3.86 mmol) and **7** (1.1 g, 7.7 mmol) in 1 M aqueous sodium carbonate (8 mL) and 1,4-dioxane (24 mL) was stirred under nitrogen atmosphere for 5 min. The resulting mixture was treated with tetrakis(triphenylphosphine)palladium(0) (0.2 g, 0.18 mmol) and stirred at reflux for 8 h. Then, the reaction was cooled and diluted with EtOAc (100 mL), and washed with brine (100 mL). The aqueous layers were extracted with EtOAc (100 mL), the combined layer was dried over Na_2SO_4 and filtered, and the filtrate was concentrated under the reduced pressure. The residue obtained was purified by column chromatography (PE/EA = 1:1) to afford **8** (0.51 g, yield 57%) as an off-white solid. To a stirred solution of compound **8** (0.2 g, 0.88 mmol) and 3-aminobenzoic acid (**9**, 0.18 g, 1.32 mmol) in DMF (5 mL) was added HBTU (0.5 g, 1.32 mmol) and DIPEA (0.23 mL, 1.32 mmol). Then the reaction was stirred at room temperature for 4 h, diluted with water (100 mL), and extracted with EtOAc (3 × 30 mL). The organic layer was dried over Na_2SO_4, filtrated and the solvent was evaporated under the reduced pressure. The residue was purified by column chromatography (CH_2Cl_2/CH_3OH = 100:8) to give target compound **11a** as a yellow solid (0.11 g, yield 35%). ^{1}H NMR (DMSO-d_6, 600 MHz) δ: 8.34 (d, J = 8.83 Hz, 1H), 8.22 (d, J = 1.02 Hz, 1H), 7.87 (dd, J_1 = 8.64 Hz, J_2 = 1.80 Hz, 1H), 7.72–7.75 (m, 2H), 7.33 (t, J = 9.36 Hz, 2H), 7.10 (t, J = 7.20 Hz, 1H), 7.03–7.05 (m, 2H), 6.71–6.73 (m, 1H), 6.48 (s, 2H). ^{13}C NMR (150 MHz, DMSO-d_6, TMS) δ: 167.54, 166.10, 161.54, 153.78, 146.32, 140.60, 140.47, 140.22, 135.32, 133.22, 131.88, 131.43, 130.21, 128.54, 128.23, 127.63, 125.34, 119.33, 117.78, 116.78. MS (ESI positive): m/z $[M+H]^+$: 346.10.

The synthetic method for compounds **11b**, **11c**, **13a**, **13b**, and **18a–e** was similar to that of compound **11a**.

TABLE 2 *In vitro* Syk inhibition activity of the target compounds **18a–e**

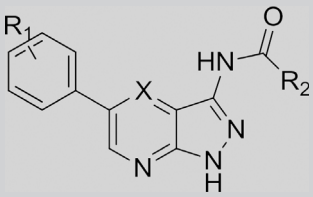

Compound	X	R_1	R_2	Inhibition rate at 5 μM (%)	IC_{50} (μM)
18a	C	3-NH_2	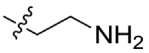	14.7	NT
18b	C	3-NH_2	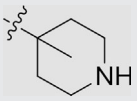	2.9	NT
18c	C	4-F	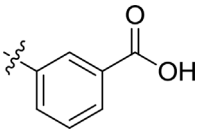	77	1.2 ± 0.04
18d	N	4-F	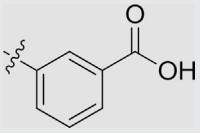	20	6 ± 0.54
18e	N	4-F	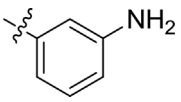	23	5.5 ± 0.36
4	–	–	–	50.3	3.2 ± 0.11

NT, not tested.

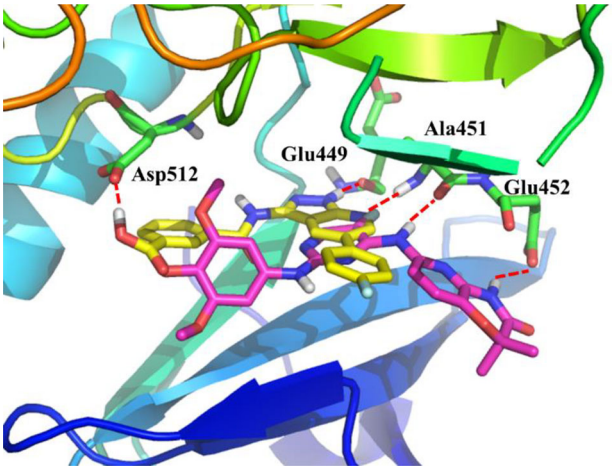

FIGURE 4 Superimposition of the binding conformation of compound **18c** and **1** in the active site of Syk-kinase. Compound carbon atoms colored in yellow for compound **18c** and in purple for compound **1**. The figure was generated using PyMol (http://www.pymol.org/)

Ethyl 3-(3-(3-aminobenzamido)-1*H*-indazol-5-yl)benzoate (11b)

Yellow solid (0.07 g, yield 60%). ^{1}H NMR (DMSO-d_6, 600 MHz) δ: 8.39 (d, J = 8.59 Hz, 1H), 8.33 (s, 1H), 8.28 (s, 1H), 8.05 (d, J = 8.13 Hz, 1H), 7.98 (d, J = 8.54 Hz, 1H), 7.95–7.99 (m, 2H), 7.67 (t, J = 7.7 Hz, 1H), 7.12 (t, J = 8.18 Hz, 1H), 6.74 (d, J = 7.78 Hz, 1H), 6.55 (s, 2H), 5.26 (s, 2H), 4.37 (d, J = 7.0 Hz, 2H), 1.34–1.37 (m, 3H). ^{13}C NMR (150 MHz, DMSO-d_6, TMS) δ: 167.67, 166.13, 153.58, 148.61, 140.71, 140.26, 135.41, 132.01, 131.20, 130.09, 129.99, 128.62, 127.57, 121.39, 119.35, 117.91, 116.91, 116.56, 115.44, 61.44, 14.67. MS (ESI positive): m/z $[M+H]^+$: 401.34.

Ethyl 3-(3-(3-(methoxycarbonyl)benzamido)-1*H*-indazol-5-yl)-benzoate (11c)

Yellow solid (0.07 g, yield 43%). ^{1}H NMR (DMSO-d_6, 600 MHz) δ: 8.43–8.48 (m, 2H), 8.16 (d, J = 7.75 Hz, 1H), 8.13 (d, J = 7.75 Hz, 1H), 7.98 (s, 1H), 7.93 (s, 1H), 7.67 (dd, J_1 = 5.88 Hz, J_2 = 7.84 Hz, 1H), 7.62 (t, J = 7.84 Hz, 1H), 6.66 (s, 1H), 4.36 (dd, J_1 = 7.03 Hz, J_2 = 7.03 Hz, 1H), 3.88 (s, 2H), 3.86 (s, 3H), 1.20 (s, 3H). ^{13}C NMR (150 MHz, DMSO-d_6, TMS) δ: 167.14, 166.14, 162.84, 154.11, 140.58, 140.13, 135.91, 135.33, 135.17, 134.23, 133.31, 132.07, 131.21, 131.21, 130.21, 131.00, 129.70, 129.32, 128.97, 128.62, 119.48, 116.67, 61.47, 52.85, 36.26. MS (ESI positive): m/z $[M+H]^+$: 444.16.

3-Amino-*N*-(5-(3-aminophenyl)-1*H*-indazol-3-yl)propanamide (13a)

Off-white solid (0.10 g, yield 85%). ^{1}H NMR (DMSO-d_6, 600 MHz) δ: 8.25 (d, J = 8.75 Hz, 1H), 8.13 (s, 1H), 7.74 (d, J = 8.52 Hz, 1H), 7.13 (t, J = 7.83 Hz, 1H), 6.87 (s, 1H), 6.81 (d, J = 7.79 Hz, 1H), 6.53–6.59 (m, 3H), 5.20 (s, 2H), 2.94–3.12 (m, 4H). ^{13}C NMR (150 MHz, DMSO-d_6, TMS) δ: 170.74, 153.37, 150.02, 149.44, 142.35, 141.29, 131.34, 129.70, 125.96, 118.32, 114.81, 112.65, 110.01, 40.56, 35.21, 28.33. MS (ESI positive): m/z $[M+H]^+$: 296.27.

N-(5-(3-Aminophenyl)-1*H*-indazol-3-yl)-4-methylpiperidine-4-carboxamide (13b)

Off-white solid (0.11 g, yield 88%). ^{1}H NMR (DMSO-d_6, 600 MHz) δ: 8.32 (d, J = 8.36 Hz, 1H), 8.16 (s, 1H), 7.76 (d, J = 8.86 Hz, 1H), 7.13 (t, J = 7.75 Hz, 1H), 6.87 (s, 1H), 6.81 (6, J = 8.49 Hz, 1H), 6.61 (s, 1H), 5.77 (s, 1H), 5.24 (s, 2H), 3.21 (s, 2H), 2.72 (d, J = 13.6 Hz, 2H), 1.89 (t, J = 12.2 Hz, 2H), 1.56 (s, 2H). ^{13}C NMR (150 MHz, DMSO-d_6, TMS) δ: 173.20, 153.04, 149.26, 140.87, 140.16, 137.67, 129.93, 129.04, 120.41, 118.85, 116.55, 115.23, 113.84, 112.91, 45.71, 42.48, 31.88, 24.36, 8.81. MS (ESI positive): m/z $[M+H]^+$: 350.27.

3-Amino-*N*-(5-(3-hydroxyphenyl)-1*H*-indazol-3-yl)benzamide (14a)

To a stirred solution of *N*-(5-(3-methoxyphenyl)-1*H*-indazol-3-yl)-pivalamide (**12a**, 0.15 g, 0.42 mmol) in CH_2Cl_2, BBr_3 (0.2 mL) was added in one portion and stirred for 6 h at −78°C. After the addition of methanol (0.4 mL) and CH_2Cl_2 (50 mL), the solution was washed with saturated $NaHCO_3$ aqueous solution (60 mL) and brine (40 mL) and dried over Na_2SO_4, and the solvent was removed under reduced pressure. The residue was purified by silica gel column chromatography (CH_2Cl_2/CH_3OH = 100:5) to afford **14a** (0.08 g, yield 55%) as yellow solid. ^{1}H NMR (DMSO-d_6, 600 MHz) δ: 9.58 (s, 1H), 8.33 (d, J = 8.47 Hz, 1H), 8.20 (d, J = 1.58 Hz, 1H), 7.82 (dd, J_1 = 8.57 Hz, J_2 = 1.80 Hz, 1H), 7.28 (t, J = 7.95 Hz, 1H), 7.08–7.13 (m, 3H), 7.03 (d, J = 7.53 Hz, 2H), 6.78 (dd, J_1 = 7.95 Hz, J_2 = 2.09 Hz, 1H), 6.71 (d, J = 7.53 Hz, 1H), 6.52 (s, 2H), 5.27 (s, 2H). ^{13}C NMR (150 MHz, DMSO-d_6, TMS) δ: 158.37, 153.61, 148.58, 141.64, 139.98, 136.78, 135.57, 130.49, 128.85, 128.60, 121.26, 118.96, 118.02, 117.91, 116.86, 116.32, 115.43, 114.89, 114.12. MS (ESI positive): m/z $[M+H]^+$: 345.36.

The synthetic method for compounds **14b** was similar to the synthesis of compound **14a**.

3-Hydroxy-*N*-(5-(3-hydroxyphenyl)-1*H*-indazol-3-yl)benzamide (14b)

Yellow solid (0.07 g, yield 48%). ^{1}H NMR (DMSO-d_6, 600 MHz) δ: 9.71 (s, 1H), 9.59 (s, 1H), 8.35 (d, J = 8.58 Hz, 1H), 8.21 (s, 1H), 7.84 (dd, J_1 = 8.58 Hz, J_2 = 1.07 Hz, 1H), 7.35 (d, J = 7.51 Hz, 1H), 7.28 (t, J = 8.04 Hz, 2H), 7.12 (d, J = 7.51 Hz, 1H), 7.09 (s,1H), 6.94 (dd, J_1 = 8.08 Hz, J_2 = 2.33 Hz, 1H), 6.78 (dd, J_1 = 8.12 Hz, J_2 = 2.08 Hz, 1H), 6.56 (s, 2H). ^{13}C NMR (150 MHz, DMSO-d_6, TMS) δ: 166.73, 158.34, 157.06, 153.78, 141.58, 139.95, 136.96, 136.02, 130.52, 129.31, 128.98, 121.13, 121.18, 118.99, 118.59, 118.05, 117.14, 116.36, 114.93, 114.12. MS (ESI positive): m/z $[M+H]^+$: 346.35.

3-Amino-*N*-(5-(3-aminophenyl)-1*H*-pyrazolo[3,4-b]pyridin-3-yl)propanamide (18a)

Yellow solid (0.06 g, yield 68%). ^{1}H NMR (DMSO-d_6, 600 MHz) δ: 8.32 (d, J = 9.39, 1H), 8.12 (s, 1H), 7.73 (d, J = 9.39 Hz, 1H), 7.13, (t, J = 7.84 Hz, 1H), 6.87 (s, 1H), 6.81 (d, J = 8.39, 1H), 6.57 (d, J = 7.95 Hz, 1H), 6.48 (s, 2H), 5.20 (s, 2H), 2.83 (s, 2H), 2.71 (d, J = 10.6 Hz, 2H), 1.63 (t, J = 8.45 Hz, 3H), 1.52 (s, 3H), 1.23 (s, 2H). ^{13}C NMR (150 MHz, DMSO-d_6, TMS) δ: 152.33, 149.67, 148.93, 147.97, 139.49, 130.02, 127.88, 127.55, 114.77, 113.22, 112.49, 108.69, 38.56, 36.25. MS (ESI positive): m/z $[M+H]^+$: 297.23.

N-(5-(3-Aminophenyl)-1*H*-pyrazolo[3,4-b]pyridin-3-yl)-4-methylpiperidine-4-carboxamide (18b)

Yellow solid (0.1 g, yield 52%). ^{1}H NMR (DMSO-d_6, 600 MHz) δ: 11.95 (s, 1H), 8.52 (d, J = 1.68 Hz, 1H), 8.27 (d, J = 1.68 Hz, 1H), 7.10 (t, J = 10.1 Hz, 1H), 6.81 (s, 1H), 6.75 (d, J = 10.1 Hz, 1H), 6.53 (d, J = 8.39 Hz, 1H), 5.61 (s, 2H), 5.17 (s, 2H), 2.57–2.71 (m, 2H), 1.45 (d, J = 4.25), 1.21 (s, 7H), 0.83 (t, J = 6.33 Hz, 1H). ^{13}C NMR (150 MHz, DMSO-d_6, TMS) δ: 152.36, 149.67, 148.92, 147.96, 139.40, 130.01, 127.92, 127.53, 114.75, 113.17, 112.48, 106.72, 29.46. MS (ESI positive): m/z $[M+H]^+$: 351.18.

3-((5-(4-Fluorophenyl)-1*H*-pyrazolo[3,4-b]pyridin-3-yl)carbamoyl)benzoic acid (18c)

Yellow solid (0.08 g, yield 52%). ^{1}H NMR (DMSO-d_6, 600 MHz) δ: 8.62 (d, J = 2.30 Hz, 1H), 8.12 (t, J = 6.41 Hz, 2H), 8.06 (d, J = 7.21 Hz, 1H), 7.78 (t, J = 6.61 Hz, 2H), 7.68 (t, J = 7.51 Hz, 1H), 7.62 (t, J = 7.51 Hz, 1H), 7.37 (t, J = 8.73 Hz, 2H), 6.75 (d, J = 2.90 Hz, 1H), 6.65 (s, 2H). ^{13}C NMR (150 MHz, DMSO-d_6, TMS) δ: 167.47, 152.29, 151.64, 149.38, 134.26, 133.94, 133.55, 132.41, 131.25, 130.95, 129.58, 129.47, 128.60, 127.93, 126.01, 116.75, 116.47, 116.20, 113.21. HRMS (ESI, positive) m/z calcd. for $C_{20}H_{14}FN_4O_3$ (M+H): 377.1044; found 377.1058.

3-((5-(4-Fluorophenyl)-1*H*-pyrazolo[3,4-b]pyrazin-3-yl)carbamoyl)benzoic acid (18d)

Yellow solid (0.05 g, yield 38%). ^{1}H NMR (DMSO-d_6, 600 MHz) δ: 12.47 (s, 1H), 9.05 (s, 1H), 8.22 (dd, J_1 = 3.55 Hz, J_2 = 5.75 Hz, 2H), 7.39 (t, J = 9.12 Hz, 2H), 5.81 (s, 2H). ^{13}C NMR (150 MHz, DMSO-d_6, TMS) δ: 167.19, 166.12, 152.19, 150.83, 144.54, 134.24, 133.44, 130.41, 130.21, 129.77, 128.52, 127.63, 126.10, 116.45, 116.23, 116.10, 113.43, 91.35. MS (ESI positive): m/z $[M+H]^+$: 378.36.

3-Amino-*N*-(5-(4-fluorophenyl)-1*H*-pyrazolo[3,4-b]pyrazin-3-yl)benzamide (18e)

Yellow solid (0.06 g, yield 65%). ^{1}H NMR (DMSO-d_6, 600 MHz) δ: 13.85 (s, 1H), 10.51 (s, 1H), 9.19 (s, 1H), 8.16–8.19 (m, 2H), 7.33 (t, J = 9.40 Hz, 2H), 7.20–7.23 (m, 2H), 7.15 (t, J = 8.05 Hz, 1H), 6.77 (d, J = 7.55 Hz, 1H), 5.30 (s, 2H). ^{13}C NMR (150 MHz, DMSO-d_6, TMS) δ: 167.74, 158.70, 149.32, 144.08, 142.15, 134.60, 131.01, 133.60,

130.94, 129.77, 129.59, 129.41, 117.96, 116.53, 116.25, 115.57, 113.71, 99.34. MS (ESI positive): *m/z* $[M+H]^+$: 349.46.

4.2 | Syk inhibition assay

The kinase assay was performed in the buffer (50 mM HEPES pH 7.5, 0.015% Brij-35, 10 mM $MgCl_2$, 10 mM $MnCl_2$, 2 mM DTT). A 5 mL volume of tested compounds were prediluted for dose response in 384-well plates. A 10 mL volume of diluted enzyme solution was sequentially added and the assay plates were incubated at room temperature for 10 min. Then a 10 mL volume of a mixture of peptide solution containing FAM-labeled peptide (Cat. No. 112396, Lot. No. P100804-XZ112396; GL Biochem, China) and ATP (Cat. No. A7699-1G, CAS No. 987-65-5; Sigma, USA) was incubated at 28°C for 25 min. Reaction was stopped with the addition of 50 mM EDTA containing 25 mL of 100 mM HEPES, pH 7.5, 0.015% Brij-35, and 0.2% Coating Reagent #3, and the data were collected on a caliper. Half maximal inhibition (IC_{50}) values were calculated using a nonlinear curve fit with XLfit software.

4.3 | Molecular docking

The crystal structure of Syk in complex with **1** was obtained from the Protein Data Bank (PDB ID: 3FQS[17]) and prepared for docking using the protein preparation tool in Discovery Studio 3.0. During the process, the ligands and waters were removed and hydrogens were added to the structure. Staged minimization was performed with the default setting. The docking studies were carried out using GOLD 5.0 because it could effectively reproduce the binding conformation of R406 with Syk (PDB ID: 3FQS) with the RMSD value of 1.1 Å.[18] Binding site was defined as whole residues within a 10 Å radius subset encompassing the compound **1**. Conformations were generated by genetic algorithm and scored using GoldScore as fitness function. The best conformation was chosen to analyze the ligand–protein interaction. The image representing the best pose was prepared using PyMol.

ACKNOWLEDGMENTS

This work was supported by the National Key R&D Program of China (2017YFA0506000) and the National Basic Research Program of China (2014CB541800).

CONFLICT OF INTEREST

The authors have declared no conflict of interest.

ORCID

Chunquan Sheng http://orcid.org/0000-0001-9489-804X

REFERENCES

[1] J. Dorais, G. Gregoire, J. LeLorier, *N. Engl. J. Med*. **1992**, *327*, 1882.
[2] Y. Pirson, C. van Ypersele de Strihou, *Am. J. Kidney Dis*. **1986**, *8*, 338.
[3] P. V. Voulgari, *Expert Opin. Emerg. Drugs* **2008**, *13*, 175.
[4] A. Mocsai, J. Ruland, V. L. Tybulewicz, *Nat. Rev. Immunol*. **2010**, *10*, 387.
[5] S. L. Tan, C. Liao, M. C. Lucas, C. Stevenson, J. A. DeMartino, *Pharmacol. Ther*. **2013**, *138*, 294.
[6] J. A. Gomez-Puerta, A. Mocsai, *Curr. Top. Med. Chem*. **2013**, *13*, 760.
[7] J. Smith, J. P. McDaid, G. Bhangal, R. Chawanasuntorapoj, E. S. Masuda, H. T. Cook, C. D. Pusey, F. W. Tam, *J. Am. Soc. Nephrol*. **2010**, *21*, 231.
[8] S. Matsubara, G. Li, K. Takeda, J. E. Loader, P. Pine, E. S. Masuda, N. Miyahara, S. Miyahara, J. J. Lucas, A. Dakhama, E. W. Gelfand, *Am. J. Respir. Crit. Care Med*. **2006**, *173*, 56.
[9] F. R. Bahjat, P. R. Pine, A. Reitsma, G. Cassafer, M. Baluom, S. Grillo, B. Chang, F. F. Zhao, D. G. Payan, E. B. Grossbard, D. I. Daikh, *Arthritis Rheum*. **2008**, *58*, 1433.
[10] L. Colonna, G. Catalano, C. Chew, V. D'Agati, J. W. Thomas, F. S. Wong, J. Schmitz, E. S. Masuda, B. Reizis, A. Tarakhovsky, R. Clynes, *J. Immunol*. **2010**, *185*, 1532.
[11] A. Podolanczuk, A. H. Lazarus, A. R. Crow, E. Grossbard, J. B. Bussel, *Blood* **2009**, *113*, 3154.
[12] M. E. Weinblatt, A. Kavanaugh, R. Burgos-Vargas, A. H. Dikranian, G. Medrano-Ramirez, J. L. Morales-Torres, F. T. Murphy, T. K. Musser, N. Straniero, A. V. Vicente-Gonzales, E. Grossbard, *Arthritis Rheum*. **2008**, *58*, 3309.
[13] S. P. McAdoo, F. W. Tam, *Drugs Future* **2011**, *36*, 273.
[14] S. Krishnan, Y. T. Juang, B. Chowdhury, A. Magilavy, C. U. Fisher, H. Nguyen, M. P. Nambiar, V. Kyttaris, A. Weinstein, R. Bahjat, P. Pine, V. Rus, G. C. Tsokos, *J. Immunol*. **2008**, *181*, 8145.
[15] Y. Huang, Y. Zhang, K. Fan, G. Dong, B. Li, W. Zhang, J. Li, C. Sheng, *Bioorg. Med. Chem. Lett*. **2017**, *27*, 1776.
[16] E. B. Kaloun, K. Bedjeguelal, R. Rabot, A. Kruczynski, P. Schmitt, M. Perez, N. Rahier, EP US94528510, **2012**.
[17] A. G. Villasenor, R. Kondru, H. Ho, S. Wang, E. Papp, D. Shaw, J. W. Barnett, M. F. Browner, A. Kuglstatter, *Chem. Biol. Drug Des*. **2009**, *73*, 466.
[18] G. Jones, P. Willett, R. C. Glen, A. R. Leach, R. Taylor, *J. Mol. Biol*. **1997**, *267*, 727.
[19] F. Padilla, N. Bhagirath, S. Chen, E. Chiao, D. M. Goldstein, J. C. Hermann, J. Hsu, J. J. Kennedy-Smith, A. Kuglstatter, C. Liao, W. Liu, L. E. Lowrie, Jr., K. C. Luk, S. M. Lynch, J. Menke, L. Niu, O. Y.C Owens, R. C. Schoenfeld, M. Slade, S. Steiner, Y. C. Tan, A. G. Villasenor, C. Wang, J. Wanner, W. Xie, D. Xu, X. Zhang, M. Zhou, M. C. Lucas, *J. Med. Chem*. **2013**, *56*, 1677.

SUPPORTING INFORMATION

Additional supporting information may be found online in the Supporting Information section at the end of the article.

How to cite this article: Huang Y, Li Y, Dong G, Zhang W, Liu N, Sheng C. Identification of pyrazolopyridine derivatives as novel spleen tyrosine kinase inhibitors. *Arch Pharm Chem Life Sci*. 2018;1–8. https://doi.org/10.1002/ardp.201800083